

Article

An Experimental Study on Bushing Formation during Friction Drilling of Titanium Grade 2 for Medical Applications [†]

Hans Vanhove * , Ecem Ozden  and Joost R. Dufloy 

Department of Mechanical Engineering, Katholieke Universiteit Leuven, Member of Flanders Make, Celestijnenlaan 300B, B-3001 Leuven, Belgium; ecem.ozden@kuleuven.be (E.O.)

* Correspondence: hans.vanhove@kuleuven.be; Tel.: +32-16-32-28-75

[†] This paper is an extended version of our paper published in Vanhove, H.; Mossay, C.; Dufloy, J. An experimental study of bushing formation during friction drilling of titanium grade 2 for medical applications. In Proceedings of the 20th International Conference on Sheet Metal (SHEMET 2023), Erlangen-Nürnberg, Germany, 2–5 April 2023; pp. 353–360.

Abstract: Recent advances towards patient specific titanium sheet based medical implants introduce a new challenge for the fixation of these implants to bones. Mainly, the use of locking screws requires an implant thickness of approximately 2 mm for screw thread formation. Friction drilling is a hole-making process that displaces material to create a bushing below the sheet rather than extracting material. This experimental study explores the influence of axial force, rotational speed, and workpiece pre-heating temperature on the bushing height and thickness during friction drilling of titanium grade 2 sheets. The drilling parameters are optimized for both drilling at room temperature and at elevated temperatures for maximum bushing thickness with at least a bushing height of 1 mm. Subsequently, the samples are characterized for their microstructure and hardness, revealing preserved strength with a larger thermomechanical affected zone (TMAZ), a more gradual hardness gradient around the drill zone, and a significant reduction in microdefects in the bushing structure of the pre-heated sheets.

Keywords: friction drilling; commercially pure titanium; medical implant; microstructure



Citation: Vanhove, H.; Ozden, E.; Dufloy, J.R. An Experimental Study on Bushing Formation during Friction Drilling of Titanium Grade 2 for Medical Applications. *J. Manuf. Mater. Process.* **2023**, *7*, 220. <https://doi.org/10.3390/jmmp7060220>

Academic Editor: Antonio Riveiro

Received: 12 October 2023
Revised: 13 November 2023
Accepted: 28 November 2023
Published: 6 December 2023



Copyright: © 2023 by the authors. Licensee MDPI, Basel, Switzerland. This article is an open access article distributed under the terms and conditions of the Creative Commons Attribution (CC BY) license (<https://creativecommons.org/licenses/by/4.0/>).

1. Introduction

The shift towards patient tailored medical care has been tangible in the advances made in research towards patient specific plate osteosynthesis. Vancleef et al. [1] have studied the potential of custom thin-walled implants for clavicle bone reconstruction. Benefits were identified on improved anatomical alignment of bone fragments, due to a better fit, while the reduced implant thickness results in less soft tissue irritation. Although thin-walled implants can reduce irritation and eliminate a potential secondary operation for implant removal, a reduced plate thickness poses a challenge towards plate fixation. While conventional osteosynthesis screws are countersunk in the implant, locking head screws use a threaded head to create angular stability to the bone fragments (Figure 1).

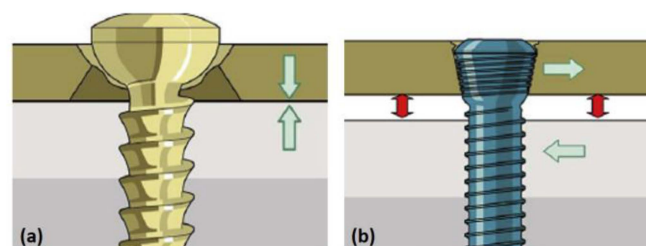


Figure 1. Medical implant fixation through: (a) conventional screws; (b) locking screws [2].

Commercial osteosynthesis locking screws have a head height of approximately 2 mm fitting the current commercial clavicle plates with a thickness varying from 2.3 to 3.4 mm. Vancleef et al. [1] have shown, however, that patient specific plates of 1.5 mm average thickness suffice to bear the loads acting on the broken bone. Thinner plates with varying thickness throughout the plate, even down to 1 mm, are the subject of ongoing research.

Friction drilling, a chip-less hole making process, provides an interesting solution to locally increase plate thickness at the fixation points [3]. The process deforms the workpiece material through friction between the conical rotating drill and the sheet, instead of removing it. The resulting upwards formed boss and downwards formed bushing can have a combined height up to four times the initial sheet thickness [4].

This process was first described in 1923 by Jan Clause de Valliere, but could only be put into practice 60 years later through the development of tungsten carbide (TC) tools [5]. Since the first experiments, research has been focusing on improving the emerging geometry of bushing and hole through optimizing process parameters. More specifically, the bushing quality can be quantified by its height and thickness and occurrence of cracks and petal formation. Ozler et al. [6] concluded that an increased *rotational speed* of the drill (ω) increases the temperature and thus lowers the yield stress, resulting in a lower thrust force. A longer bushing height is accompanied by a thinner bushing and reduced petal formation as a result of the increased forming temperature.

Most research has been performed using a constant *feed rate* (f), letting the thrust force vary throughout the different stages of friction drilling a hole [7]. The contact time between drill and sheet reduces with increased feed rate, resulting in a higher thrust force and tool torque. An increased roughness, shortened but thicker bushing, and increased petal formation and cracks are the main effects on the final hole [7]. The presented work here, however, uses a *constant thrust force* and thus the forming speed varies as the drill sinks through the sheet.

Moreover, friction drilling technology, currently under evaluation for novel applications due to its thermal effects during the process, can be utilized to join both similar and dissimilar materials [8–11]. Nevertheless, according to Eliseev et al. [12], friction drilling of single non-ferrous and steel alloy sheets currently poses no significant technological challenges; however, the situation differs significantly when drilling titanium and its alloys. The challenging nature of friction drilling for titanium and its alloys is attributed to their high strength and low thermal conductivity, often resulting in significant internal structural damage [13]. Additionally, the isolation and accumulation of temperature in the tool/sheet contact zone is known to cause local melting and the formation of extremely long and thin bushings for titanium alloys [14]. The high workpiece temperature in an oxygen rich environment results in the formation of titanium oxides which drastically increases drill wear through adhesion and abrasion [4]. In light of these challenges, Eliseev et al. [12] proposed obvious ways to improve friction drilling, especially for titanium alloys, which includes the selection of new tool configurations and coatings, as well as the utilization of supporting means such as additional heating/cooling sources and special dies. Dehghan et al. [4] investigated the effects of rotational speed and feed rate on bushing geometry, hardness, and tool wear in friction drilling of the titanium alloy Ti-6Al-4V. It was noted that low rotational speed and feed rate produced better bushing geometry, prolonged tool life, and reduced hardness in the bushing. Furthermore, the low thermal conductivity of Ti-6Al-4V may lead to excessive frictional heat and surface temperature, resulting in unsatisfactory bushing formation. The study by Pangjundee et al. [15] on friction drilling of Ti-6Al-4V showed that an increase in rotational speed and a decrease in feed rate resulted in reduced thrust force and torque. Kumar et al. [16] developed an experimentally validated thermo-mechanical finite element (FE) model to investigate Ti-6Al-4V friction. The authors observed that the maximum temperature could reach up to 604.2 °C, primarily depending on cutting speed and heat accumulation within the drilled hole. Kumar and Hynes [17] also built another FE model for Ti-6Al-4V alloy friction drilling to predict strain, stress, and temperature distributions. It was likewise observed that the maximum temperature could reach up to

797.7 °C, which is below the melting point of the material. However, the numerical findings necessitate validation through experimental studies.

In contrast to the recent research on friction drilling of Ti-6Al-4V alloy, friction drilling studies on commercially pure titanium are severely limited. Miller et al. [13] investigated friction drilling of steel, aluminum, and commercially pure titanium. The authors concluded that friction drilling of commercially pure titanium is the most challenging, producing short and thick bushings. Particularly, titanium grade 2 is the most used commercially pure titanium for medical applications due to its excellent strength to weight ratio, biocompatibility, high corrosion resistance, lack of magnetic attraction, and wide availability. In addition to its various advantages, titanium grade 2 stands out due to its elemental purity, offering superior biocompatibility and non-cytotoxicity [18]. This is achieved by excluding elements such as Al and V, which have recently raised concerns in commonly used biomedical implant materials.

Despite the extensive research on friction drilling, there is a remarkable lack of literature on optimizing the bushing structure for titanium grade 2. This publication addresses this gap by exploring how pre-heating the workpiece, specifically commercially pure titanium grade 2 (CP-Ti Grade 2), affects the bushing structure. This experimental study aims to investigate three main aspects: the bushing geometry and its associated process parameters, the effects of pre-heating on microstructure, and the resulting mechanical properties. The fundamental concept is that a larger heated zone will facilitate the superplastic deformation of the material as it flows from the sheet into the bushing.

2. Materials and Methods

A commercially pure titanium grade 2 rolled and annealed sheet is chosen as workpiece material. The samples are 20 × 60 mm with a thickness of 1mm. Table 1 presents the chemical composition of titanium grade 2, classified according to the ASTM B265 standard [19].

Table 1. Chemical composition of titanium grade 2 [19].

| CP-Ti Grade 2 | Chemical Composition [weight-%] | | | | | |
|---------------|---------------------------------|------|-------|-----|------|---------|
| | N | C | H | Fe | O | Ti |
| | 0.03 | 0.08 | 0.014 | 0.2 | 0.17 | Balance |

The friction drilling process uses a 3.7 mm friction drill (Flowdrill M04–3.7 Long standard). It is made of tungsten carbide in cobalt matrix and has a friction angle of 36°. Berulit 935 is selected as lubricant for its high temperature stability (up to 950 °C), in order to reduce tool wear. The tool is dipped into the berulit 935 immediately prior to the forming of each hole. Moreover, the drill is also cleaned after each use with a steel wire brush to remove any titanium adhesion to the tool.

Drilling is performed on an Alzmetal Drill press, offering a wide variety of rotation speeds. It is equipped with an actuation disk that allows attachment of different weights to provide a constant thrust force on the drill. Figure 2 depicts the experimental platform.

A custom-designed heating platform has been mounted on the bed of the table drill in order to heat the titanium sheet before and during drilling. The platform is manufactured in house from S235 JR and is heated by two Vulcanic© Vulstar 1007-26 cartridge heaters. Applying a thermal paste between the platform and heating elements ensures efficient thermal conductivity. Insulation layers are applied at the top and bottom of the platform to prevent the heat from flowing to the machine. Due to the high thermal inertia of the solid heating block, it is kept at constant temperature throughout tests using a PID controller receiving temperature feedback by a K-type thermocouple placed in the center of the block. Interchangeable steel clamping plates of 120 × 50 × 6 mm with a low thermal capacity are used to clamp the Titanium sheet and can be mounted on the steel heating platform. Figure 3 shows a CAD drawing of the heating platform. An 8 mm hole in the clamping

plate provides space for the drill to penetrate through the sheet, simultaneously serving as support of the sheet to confine the plastic deformation zone.

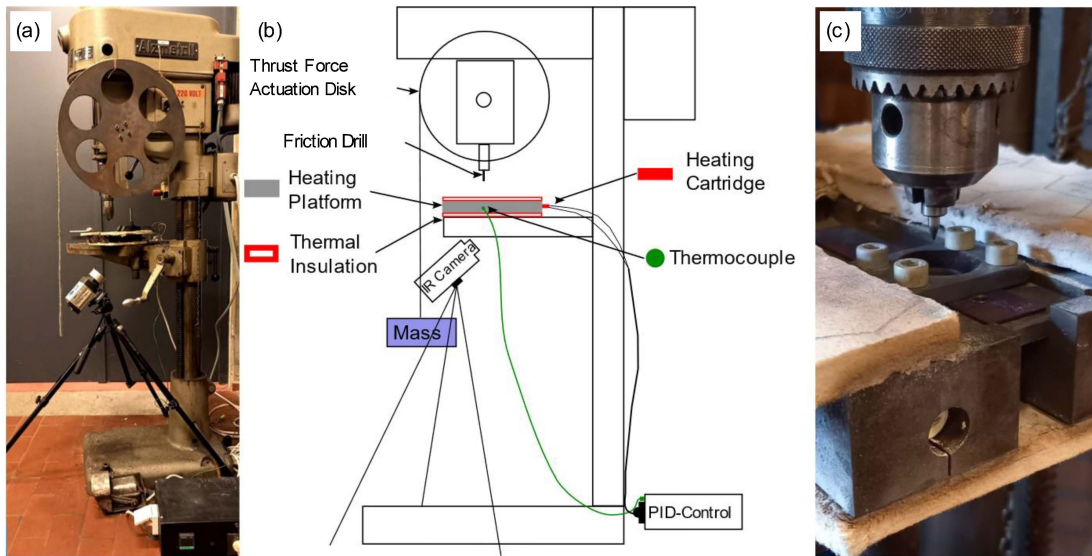


Figure 2. Friction drilling platform: (a) lab setup; (b) schematic representation; (c) closeup of the friction drill and heating platform.

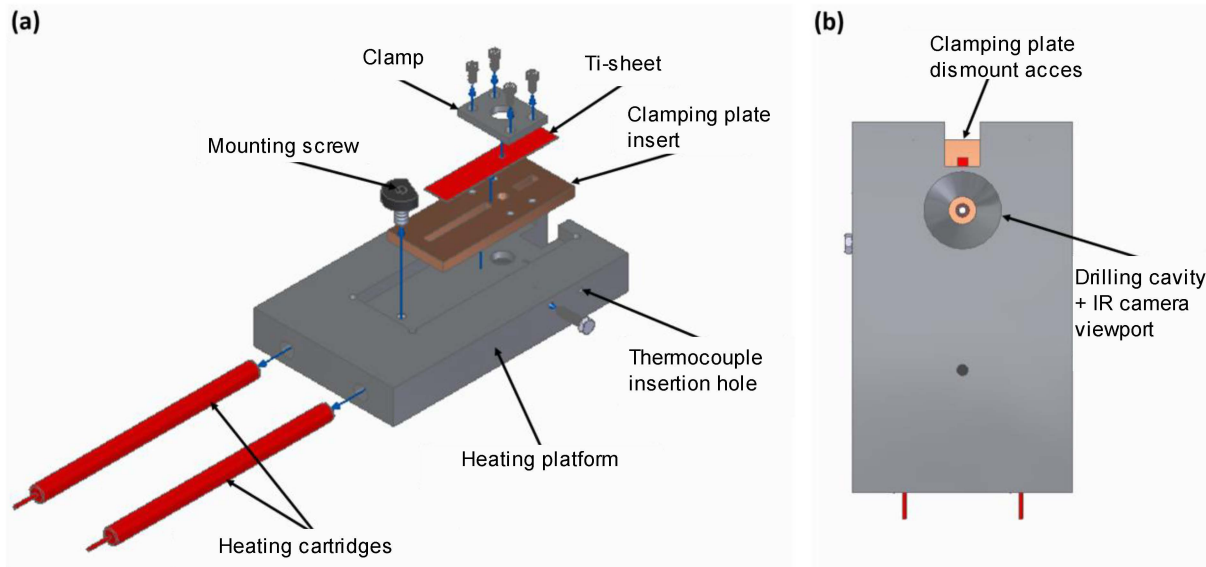


Figure 3. CAD drawing of the heating platform: (a) exploded view; (b) bottom view.

In addition to using a thermocouple to control the heating block temperature, a FLIR Thermovision A20 IR camera is set up to monitor the temperature of the backside of the sheet. A secondary thermocouple at the middle of the drilling location at the front of the titanium sheet is used to verify the correct pre-heating temperature. Once a steady state is confirmed (15 min), the thermocouple is removed and drilling starts.

The bushings are analyzed using a Nikon© LC 60 Dx (Nikon) laser scanning probe, mounted on a Coord3 CMM. The resulting point clouds allow to quantify the bushing height and thickness. The total hole length, which corresponds to the effective length for thread cutting, is determined by adding the bushing height to the 1 mm thickness of the titanium grade 2 sheet, as shown in Figure 4. Thickness measurements are performed at 1 mm from the back of the sheet, thus at a 1 mm bushing height. As possible cracks or petal

formation cause variation of height and thickness along the circumference of the bushing, the bushing height is defined as the minimum crack-less height measured. The thickness is defined as an average thickness, taken along the circumference of the 1 mm mark for the remainder of this paper (Figure 4).

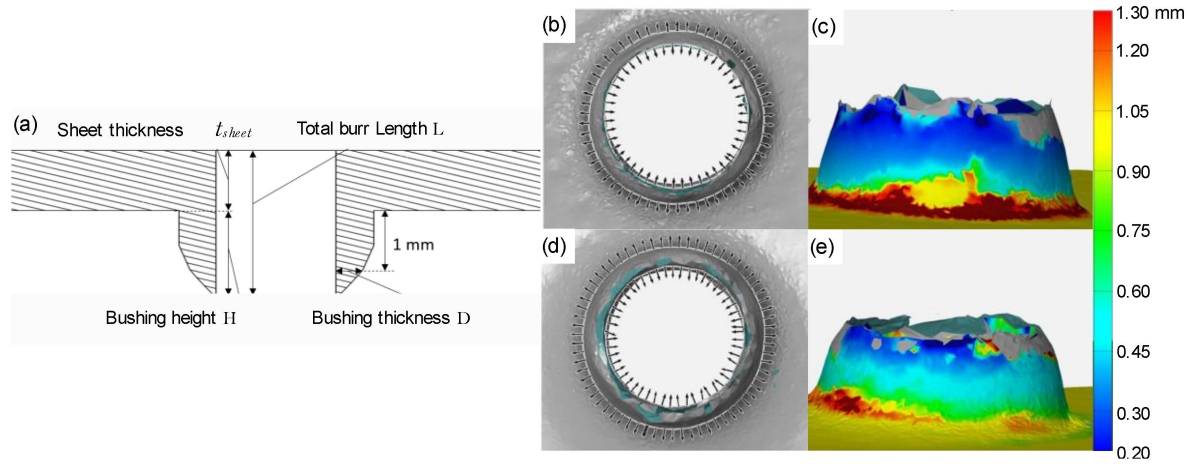


Figure 4. (a) Dimensions nomenclature for friction drilling in this paper; (b,c) thickness measurement of a friction drilled hole at room temperature with optimal drilling parameters; (d,e) thickness measurement of a pre-heated friction drilled hole with optimal drilling parameters.

The thrust force, rotational speed, and workpiece pre-heating temperature are variables considered in a factorial analysis varying between two levels. The thrust force is limited on the lower side by a lack of penetration while the upper boundary is defined by premature breakage of the bushing. Both cases are most stringently limited when no pre-heating is used. Similarly, the absence of penetration through insufficient heating defines the bottom limit of the rotational speed. The upper limit here, however, is constrained by machine capacity. The table drill used for the experiments has a maximum rotation speed of 2800 rpm. Finally, the lower- and upper- limit for the variable workpiece pre-heating are, respectively, the room temperature (20 °C) and the highest stable temperature the described setup can achieve (525 °C). Table 2 summarizes the input parameters for the factorial analysis for which all tests were performed five times.

Table 2. Variable levels for factorial analysis.

| | Lower Limit | Upper Limit |
|------------------------|--------------------------|-------------|
| Temperature [°C] | 20 °C (Room temperature) | 525 °C |
| Thrust force [N] | 361 | 722 |
| Rotational speed [rpm] | 1400 | 2800 |

The optimal drilling parameters were obtained through the method of steepest ascend for both the experiments at room temperature and elevated temperature, and were analyzed for microstructure and hardness. These two parameters sets are summarized in Table 3 and named according to the setpoint temperatures at the onset of friction drilling, the specimens mentioned in this article are the room-temperature, and the pre-heated conditions. The pre-heated sheets were heated to a temperature of 525 °C, with a 15 min holding time. Subsequently, the bushing is formed in less than a minute, followed by a 5 min holding time after drilling and air-cooling to room temperature. This heating temperature allows for both heat conduction and recrystallization, while still being low enough to prevent the bushing from melting or softening significantly during a short drilling process to a 1 mm thick sheet. Pre-heating also allows to raise the thrust force. Hence, an optimal thrust force

of 1017 N was found beyond the limits of friction drilling at room temperature and the values chosen for the factorial analysis.

Table 3. Optimal drilling parameters.

| | Room-Temperature | Pre-Heated |
|------------------------|------------------|------------|
| Temperature [°C] | 20 °C | 525 °C |
| Thrust force [N] | 722 | 1017 |
| Rotational speed [rpm] | 1400 | 1400 |

The microstructural analyses are carried out using optical microscopy (OM) and Scanning Electron Microscopy (SEM), with a focus on comparing the pre- and post-drilling characteristics of the sheets drilled at 20 °C and 525 °C. Samples are prepared by cutting the workpiece in half by means of wire electrical discharge machining, followed by embedding in a conductive resin. The cut samples are ground with SiC papers and polished with a solution consisting of 70% oxide suspension (OP-S, Struers) and 30% hydrogen peroxide (H₂O₂). The samples are etched using a 20% hydrofluoric acid solution for 3 min. To minimize charging effects, the etched samples are sputter-coated with Pt, using a Quorum Q150T/S sputter coater, and are finally evacuated for 12 h under vacuum. The microstructure is analyzed using a SEM (XL30-FEG, Philips) with an accelerating voltage of 10 kV, both for the secondary electron (SE) and backscattered electron (BSE) imaging modes. A compositional analysis is conducted by SEM (XL30-FEG, FEI) with associated EDX, EDAX using an accelerating voltage of 20 kV. For quantitative microstructural examination, light optical microscopy (Leica Laborlux, Wetzlar, Germany) with image analysis software (AxioCam MRc5, Zeiss, Germany) is used.

Correlating microstructural findings with the mechanical properties is performed using a set of hardness measurements on predetermined points along the cross-section of the friction drilled hole of the same samples prepared for SEM analysis. A Shimadzu HMV-2000 micro-hardness measuring platform (Shimadzu Corporation, Tokyo, Japan) with Vickers (HV) indenter is used with 500 g load for 15 s of dwelling time. Figure 5 shows the indent locations along the bushing and the sheet surrounding the hole. A total of five indents have been made for each sample respecting the proper distance from the side as well as from each other. Finally, the indents are measured using a Hirox KH-8700 (Hirox, Tokyo, Japan) digital microscope.



Figure 5. Cross-sectional hardness measurements: (a) locations of indents; (b) close-up of an indent.

3. Results and Discussion

The factorial analysis focuses on the total hole length and bushing thickness as responses. A minimal total crack-less hole length of 2 mm is envisioned in order to contain the total locking screw head. Longer bushings are acceptable as they can be ground down to the correct length. The thickness should, however, be as large as possible for structural purposes.

All experiments were performed 5 times and had a minimal bushing height (H_{min}) of 1 mm, resulting in a total hole length exceeding 2 mm. The interval plot in Figure 6 depicts a 95% confidence interval for the minimal bushing height. A trend of increasing bushing

height can be observed with increasing rotational speed and increasing workpiece pre-heating temperature. Both will increase the final total workpiece temperature, improving superplasticity. The effect of increased thrust force is, however, less obvious as rising the thrust force increases the occurrence of cracks. A higher thrust force also increases the forming speed and lowers the superplastic effect.

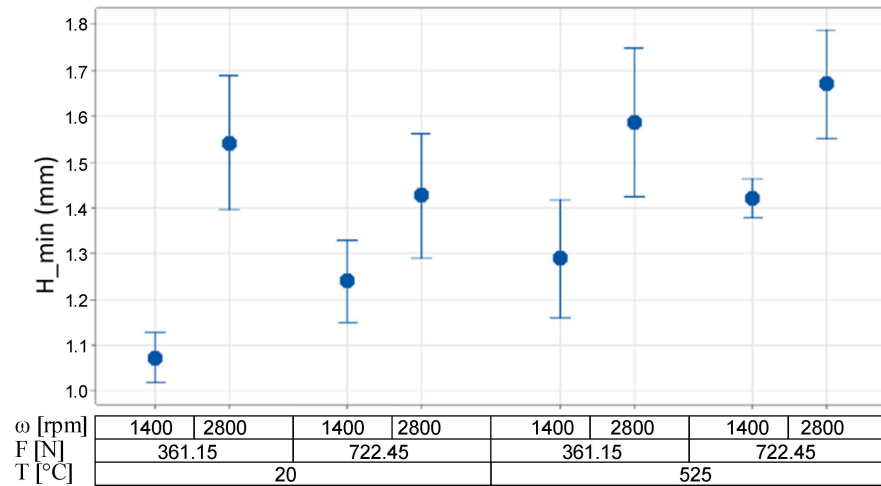


Figure 6. Interval plot of the minimal bushing height.

As all experiments fit the requirement of minimal 1 mm bushing height, the thickness can be analyzed using Minitab. The Pareto graph shown in Figure 7 shows the thrust force (F) as the most significant variable for determining the bushing thickness. It is followed by the workpiece pre-heating temperature (T), the temperature-thrust force interaction (T·F), and rotational speed (ω). The thrust force-rotational speed interaction barely crosses the significance line, while other interactions are deemed not significant.

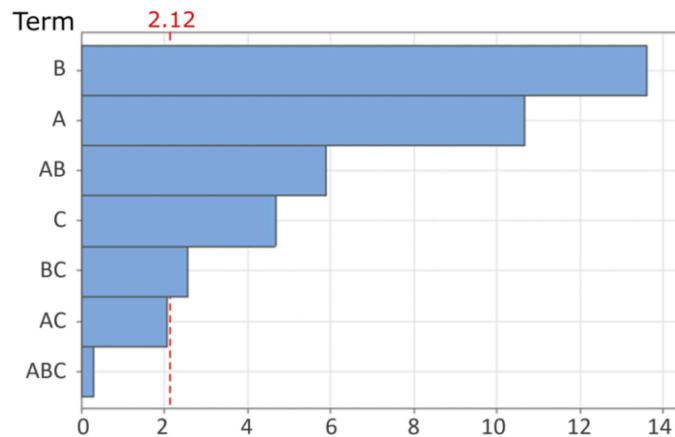


Figure 7. Pareto chart of the standardized effects for bushing thickness.

An analysis of the significant effects shows a considerable increase in bushing thickness when increasing the workpiece pre-heating temperature. This was expected as pre-heating the sheet reduces the temperature gradient and aids in increasing the volume of material at elevated temperature, which is thus subjected to superplastic forming. An increase of thrust force also has a beneficial effect on the bushing thickness and follows earlier observations described in literature [6], where an increased feed rate (and accompanying thrust force) resulted in thicker bushings due to the increased radial force applied on the material. This, however, also causes shorter bushings and an increased probability of crack formation as negative side effects. The rotational speed has a reducing effect on the bushing thickness

due to its higher temperature, which results in an enhanced material flow into a longer bushing, at the cost of bushing thickness.

Figure 8b shows a clear interaction between workpiece pre-heating and thrust force. The effect of temperature increase is much more pronounced at high thrust force than at low thrust force. This again confirms the effect on bushing thickness of involving more material in the plastic deformation. Figure 4 shows the difference in bushing thickness of drilling at 20 °C and 525 °C. Where the bushing drilled at room temperature has a steep thinning gradient at its base, the bushing drilled at elevated temperature shows a more gradual decrease in thickness along the bushing height.

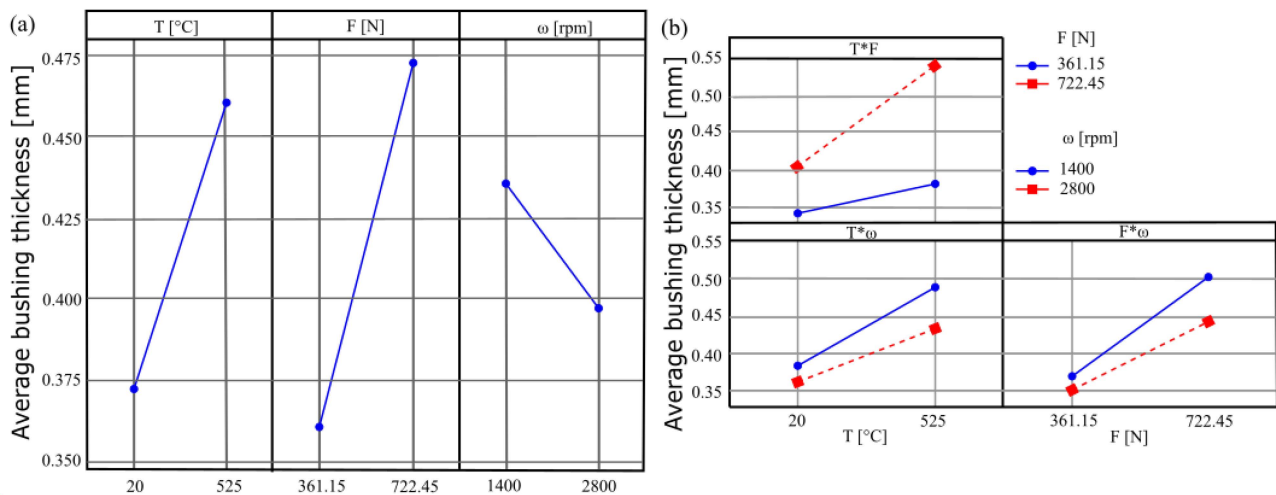


Figure 8. Bushing thickness: (a) main effects; (b) 2nd order interaction effects.

A reverse and reduced interaction can be seen for $T \cdot \omega$ and $F \cdot \omega$. In these cases, the effect of workpiece pre-heating and thrust force respectively are reduced when the rotational speed is increased.

Microstructural analysis is performed on both room temperature and elevated temperature drilling sheets (see Table 3). Initially, the microstructure before friction drilling is investigated to assess their respective properties. The production background of the as-received sheet includes processing in a vacuum furnace, hot rolling, and subsequent annealing under standard conditions. To investigate the base material at the pre-heated condition, the as-received sheet is also heated to 525 °C, and the same temperature used during the friction drilling process. It is then held at this temperature for 20 min before being air-cooled to room temperature, resulting in a modified version of the as-received sheet. The chemical composition of both as-received and pre-heated sheets is found to be identical, without any phase transformation. The EDX analysis revealed that both sheets have major amounts of Ti with hexagonal close-packed crystal structure (alpha phase), along with minor amounts of C, Fe, O and N elements and they primarily exist as precipitates at the grain boundaries and within the grains, especially near the grain boundaries. Furthermore, no other crucial precipitate formations are observed such as Ti, TiNi, and TiCrFe, which would typically enhance the twin bonding structure [20].

Figure 9a depicts the optical micrograph of the as-received sheet with its grain size distribution. After rolling and annealing, mostly equiaxed grains are observed, with an average grain size of 15.9 μm. The pre-heated sheet has similar characteristics, but with a remarkable frequency of grain sizes ranging from 0.5 to 5 μm (Figure 9b) which is rarely observed in as-received sheet. This is due to the start of recrystallization, a formation of equiaxed grains that start growing as small nuclei in areas of higher free energy density, particularly grain boundaries [21]. With sufficient time, these grains will completely replace the original matrix. However, here, the holding time is only as long as the parts used in the friction drilling process (20 min), resulting in the observation of partially recrystallized grains located at the grain boundaries. Although grain growth is also observed in pre-

heated sheet, the average grain size decreases to $14.5\ \mu\text{m}$ due to the share of partially recrystallized grains, as shown in Figure 9b.

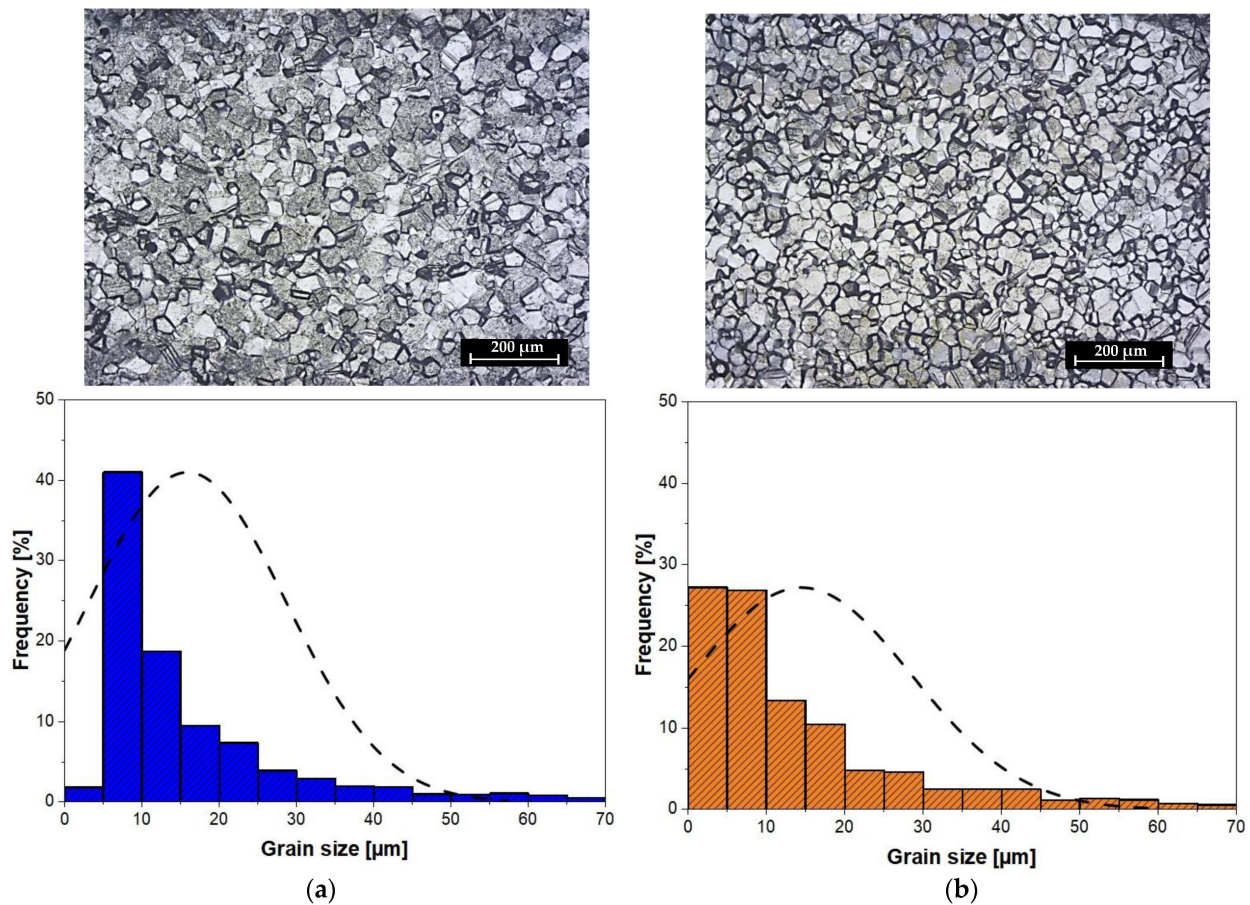


Figure 9. Optical micrograph and histogram with log-normal fit of the grain size distribution: (a) as-received sheet; (b) pre-heated sheet.

The mechanism of the friction drilling process is known to share similarities with friction stir welding [22]. These similarities have allowed the adoption of the terminology used in friction stir welding for the different structural zones in several friction drilling studies [22–25]. These zones are typically described along the cross-section of a part, extending from the drilled section towards the least affected areas. The zones, in sequential order, are the drilling zone (DZ), also known as stir zone (SZ), which is subjected to severe plastic deformation and elevated temperatures as it interacts with the tool; the thermomechanically affected zone (TMAZ), where the material undergoes deformation and elevated temperatures despite not being in direct contact with the tool; the heat affected zone (HAZ), primarily influenced by the thermal aspects of the process; and finally, the base material (BM) structure [22].

Figure 10 represents cross-sectional images of the right side of the drilled hole at the room temperature and the pre-heated processing conditions, highlighting their estimated structural zones. These zones are classified primarily based on the grain size distribution and grain orientation.

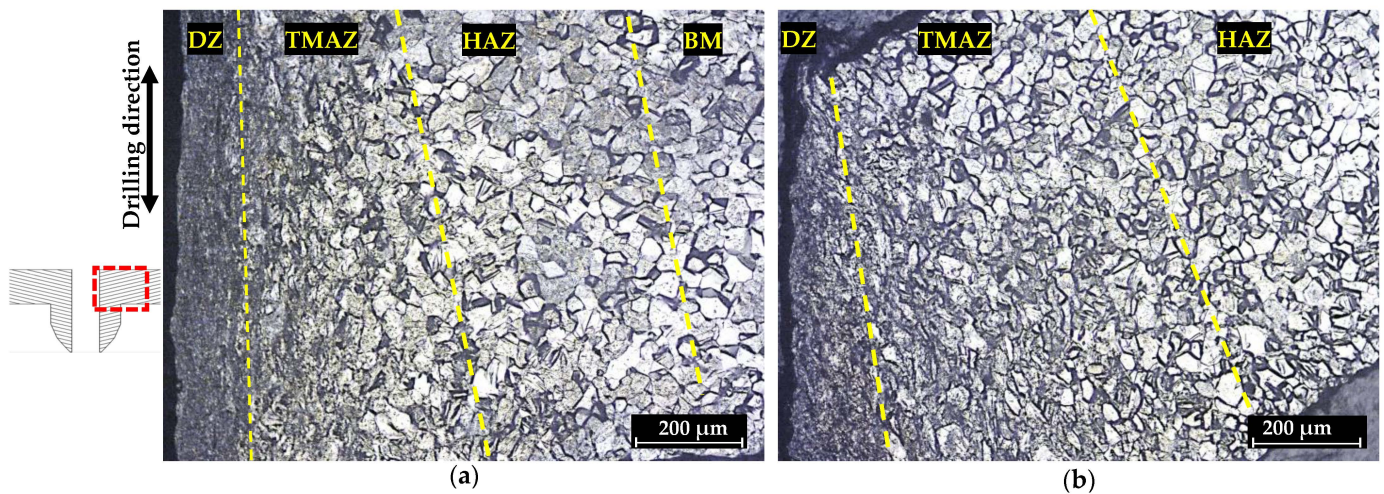


Figure 10. Cross-sectional optical micrograph and the classified friction drilling structure zones, drilling at: (a) 20 °C; (b) 525 °C.

When compared to the pre-heated sheet, the structural characteristics of drilling at room temperature exhibit several noteworthy differences. Firstly, the DZ of the room-temperature drilled sheet exhibits a narrow-walled shear-dominated structure with a distinct structural contrast at the interface between the DZ to TMAZ (Figure 10a). In contrast, the pre-heated sheet shows no clear identifiable boundary between the DZ and TMAZ, just like the interfaces in other sections (Figure 10b). Secondly, the total impact area of friction drilling structures in the pre-heated sheet is significantly larger than that in the room-temperature sheet, particularly in the TMAZ. These differences are attributed to the high strength and low thermal conductivity of Ti Grade 2 at room temperature, which leads to more localized strain within a narrow area. In other words, the dissipation of the heat produced by friction drilling is restricted due to the low thermal conductivity at room temperature. When pre-heating the sheet, the temperature gradient is much more gradual and thus the mechanically and thermal affected zones are larger and more gradual with less distinct borders.

While the investigation in the DZ will be discussed later, within the TMAZ of both sheets, elongated grains, particularly oriented in the drilling direction, are observed along with remarkable localized deformation regions. In accordance with the study by Eliseev et al. [22], grains are larger than those in the base material, both longitudinally and transversely, as a consequence of grain growth in both sheets. In the room-temperature drilling, partial recrystallization is only evident near the DZ, whereas in the pre-heated drilling, it is observed to a greater extent along the TMAZ. It should be noted here that recrystallization is already observed in the pre-heated sheet at 525 °C, as described in Figure 9b, while higher temperatures are reached during friction drilling. The transition from the HAZ to the BM is not marked and evaluated in this study. However, the transition line between the TMAZ and HAZ is illustrated in Figure 10.

Figure 11 shows the DZ at the two different bushing distances from the front surface of the sheet, along the drilling direction. At a 1 mm distance, the areas of intense shear clusters become evident in the bushing. These clusters are defined by an almost parallel orientation with the drilling direction. However, due to the up and down movement inherent to the friction drilling process, perfect parallelism is not maintained, resulting in the appearance of spiral patterns or swirls [13]. This can result in a cluster of cracks due to stress concentration and thermal stress [13]. Especially in room-temperature drilling, severe microcracks are observed, such as the areas indicated by the red arrows and a 15 μm long microcrack labelled as a box in Figure 11. Pre-heating, on the other hand, has positive effects, as only a few microcracks not larger than 2 μm are observed. Moreover, although recrystallization is observed for both sheets at a 1 mm distance from the front of

the sheet, the pre-heated sheet showed dynamic recrystallization (DRX)-rich areas where the shear stress is notably reduced. Here, it could be estimated that the DRX-rich areas formed intense shear clusters during friction drilling at a certain point in time. At a 2 mm bushing distance, the temperature is much higher than at the 1 mm bushing, leading to a predominance of mostly recovered structures in both sheets.

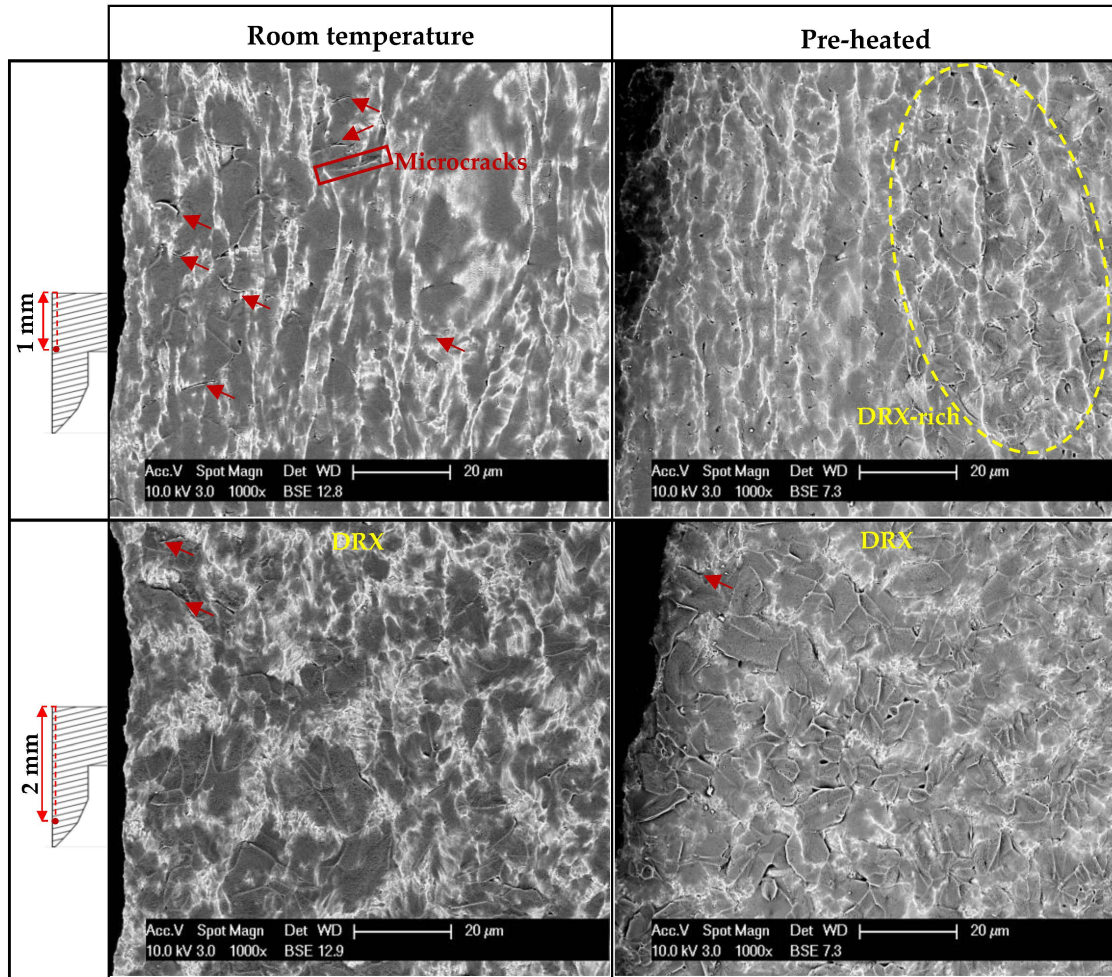


Figure 11. SEM images along the bushing under room temperature and pre-heated drilling conditions.

Figure 12 shows a close examination of the bushing structure at 1 mm along the drilling distance. The drilling at room-temperature microstructure exhibits shear bands that often have shear defects, as well as intergranular cracking along the boundaries (Figure 12b). This type of microstructure is often associated with a decrease in fatigue life. On the other hand, the pre-heated drilling has already undergone recovery compared to the room-temperature drilling, which prevents severe micro defects.

To sum up, pre-heating has a beneficial effect on the bushing structure, resulting in a strong DRX structure with the reduction of shear effects. This, in turn, helps reduce defects such as shear, twinning, and intergranular cracking, which are observed in the microstructure of the room-temperature drilled condition.

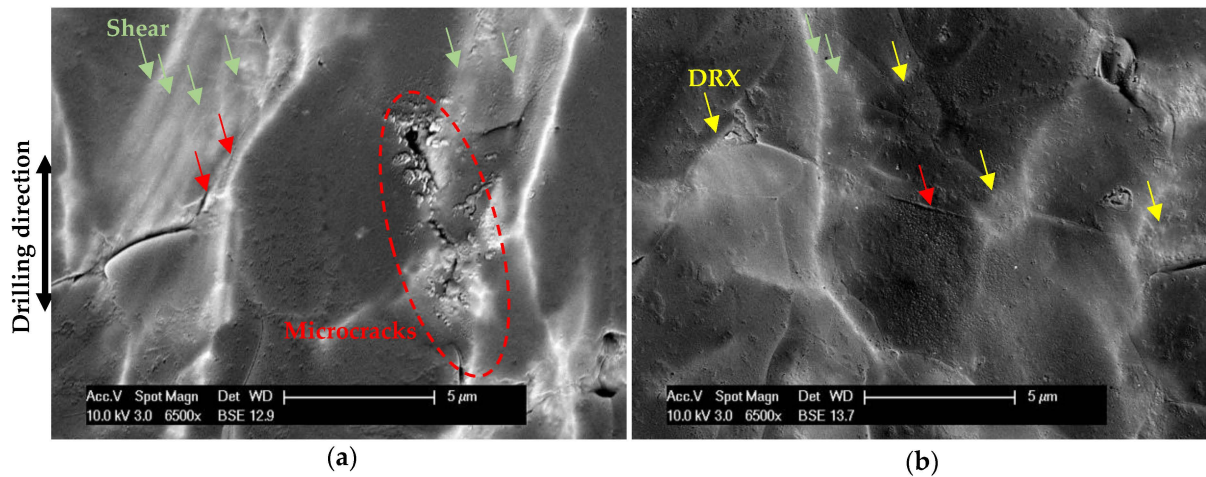


Figure 12. SEM images of bushing structures at 1 mm distance drilled at: (a) 20 °C; (b) 525 °C.

Hardness measurements are performed on at five points: three along the horizontal axis and three along the bushing, sharing the corner point (Figure 5). The average hardness values of five different repeated samples at these points with their standard deviations are presented in Figure 13. Figure 13b shows the hardness values at different horizontal distances from bushing to the base material. In accordance with the microstructural findings detailed in Figure 10, indentation points at 0.25 mm, 1 mm, and 3 mm correspond to the following regions at pre-heated condition: DZ-TMAZ, TMAZ, and HAZ, respectively. In contrast, at room temperature, the 0.25 mm indentation point is in the DZ, and the 1 and 2 mm indentation points are in the HAZ (or BM), respectively. The compatibility of these findings with the hardness values becomes more evident at a distance of 1 mm. At this distance, the room-temperature sheet has a hardness value similar to that at a distance of 3 mm, with no evidence of strain hardening. Conversely, the pre-heated sheet has a remarkable increase in hardness, providing a clear indication of thermomechanical influence. This further confirms that the drilled sheet at room-temperature is only substantially affected by strain hardening within a very limited area, while the pre-heated drilling is affected in a larger area with a more linear distribution.

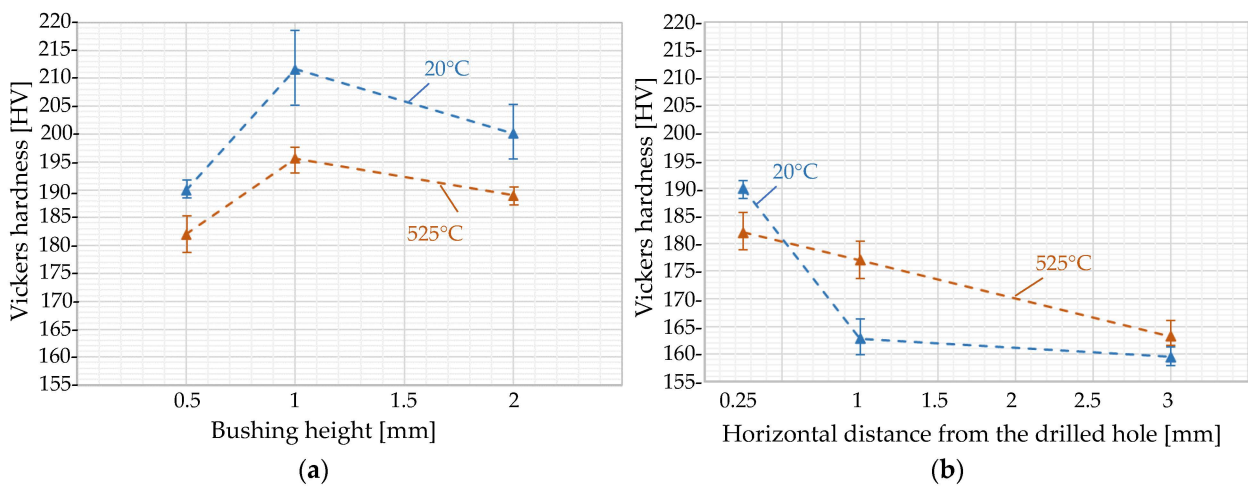


Figure 13. Vickers hardness profiles of the sheets: (a) along the bushing and (b) along the surrounding sheet.

Another noteworthy observation from Figure 13b is that the surface at a distance of 3 mm, exhibited similar hardness characteristics in both sheets. Importantly, as de-

sired, no significant softening is observed on the pre-heated sheet, despite the presence of recrystallization, as shown in Figure 9b.

The hardness along the bushing shows a similar trend between pre-heated and room-temperature drilling sheets at the measured points. In both cases, the measured hardness is higher at the 1 mm location than in the 0.5 mm corner point and the 2 mm point further down the bushing (Figure 13a). The room-temperature drilling bushings have a higher hardness throughout the bushing than the pre-heated ones. Moreover, the decrease in hardness from 1 mm to 2 mm distance is consistent with the findings in Figure 11, which indicates that recovery is more prominently observed at a 2 mm distance than at 1 mm in both sheets.

4. Conclusions

This paper summarizes an explorative study on the influence of rotational speed, thrust force, and pre-heating on the bushing formation in friction drilling of grade 2 titanium. It has been shown that the use of pre-heating has a positive influence on both bushing height as well as bushing thickness. An increased thrust force mainly has a varying effect on the crack free bushing height due to increased occurrence of cracks. It is, however, beneficial for the bushing thickness. Increasing the rotation speed induces more heat into the sheet tool contact zone, resulting in higher but thinner bushings for titanium grade 2. The optimal parameters for Ti grade 2 of 1 mm thickness, found in this study, are summarized in Table 3.

Particular investigations into the friction drilling at elevated temperature show transformative structural benefits that could significantly overcome challenges associated with titanium. The key to achieving these benefits lies in pinpointing the ideal pre-heating temperature and friction drilling parameters while also investigating their impact on the structure. By finding the optimal pre-heating temperature, the strength of the material could be preserved significantly without the risk of melting or phase transformation during friction drilling. The pre-heating temperature of 525 °C demonstrates that this goal is largely met. Microstructural and hardness results revealed that the sheet that has been friction drilled at room temperature exhibits a narrow-walled shear-dominated structure with a distinct structural contrast near the bushing, while the pre-heated sheet is spread over a larger area in a relatively linear distribution. In addition, microdefects in the bushing structure have been significantly eliminated due to the fact that recrystallization is more dominant on pre-heated sheets.

Future work will focus on the mechanical characterization of the bushings, thread cut into them, and strength and stiffness of the connection with the medical locking screws.

Author Contributions: Conceptualization, H.V.; methodology, H.V.; formal analysis, H.V. and E.O.; investigation, H.V. and E.O.; writing—original draft preparation, review and editing, H.V. and E.O.; visualization, H.V. and E.O.; supervision, J.R.D.; funding acquisition, H.V. and J.R.D. All authors have read and agreed to the published version of the manuscript.

Funding: The study performed in collaboration with a master thesis student Caroline Mossay in the framework of the STIFF project, facilitated by the KU Leuven C2 research fund.

Data Availability Statement: Data are contained within the article.

Conflicts of Interest: The authors declare no conflict of interest.

References

1. Vancleef, S.; Wesseling, M.; Duflou, J.R.; Nijs, S.; Jonkers, I.; Vander Sloten, J. Thin patient-specific clavicle fracture fixation plates can mechanically outperform commercial plates: An in silico approach. *J. Orthop. Res.* **2021**, *40*, 1695–17006. [[CrossRef](#)] [[PubMed](#)]
2. Szypryt, P.; Forward, D. The use and abuse of locking plates. *Orthop. Trauma* **2009**, *23*, 281–290. [[CrossRef](#)]
3. Kumar, R.; Jesudoss Hynes, N.R. Thermal drilling processing on sheet metals: A review. *Int. J. Lightweight Mater. Manuf.* **2019**, *2*, 193–205. [[CrossRef](#)]
4. Dehgan, S.; Ismail, M.I.S.; Ariffin, M.K.A.; Baharudin, B.T.H.T. Experimental investigation on friction drilling of Titanium alloy. *Eng. Solid Mech.* **2018**, *46*, 135–142. [[CrossRef](#)]

5. France, J.E.; Buick Davison, J.; Kirby, P.A. Strength and rotational stiffness of simple connections to tubular columns using flowdrill connectors. *J. Constr. Steel Res.* **1999**, *50*, 15–34. [[CrossRef](#)]
6. Ozler, L.; Dogru, N. An experimental investigation of hole geometry in friction drilling. *Mater. Manuf. Process.* **2013**, *28*, 470–475. [[CrossRef](#)]
7. Kaya, M.T.; Aktas, A.; Beylergil, B.; Akyildiz, H.K. An experimental study on friction drilling of st12 steel. *Trans. Can. Soc. Mech. Eng.* **2014**, *38*, 319–329. [[CrossRef](#)]
8. Su, K.Y.; Welo, T.; Wang, J. Improving Friction Drilling and Joining through Controlled Material Flow. *Procedia Manuf.* **2018**, *26*, 663–670. [[CrossRef](#)]
9. Dehghan, S.; Abbasi, R.; Baharudin, B.T.H.T.B.; Mousavi, M.L.; Soury, E. A Novel Approach to Friction Drilling Process: Experimental and Numerical Study on Friction Drill Joining of Dissimilar Materials AISI304/AL6061. *Metals* **2022**, *12*, 920. [[CrossRef](#)]
10. Iqbal, A.; Zhao, G.; Zaini, J.; Gupta, M.K.; Jamil, M.; He, N.; Nauman, M.M.; Mikolajczyk, T.; Pimenov, D.Y. Between-the-holes cryogenic cooling of the tool in hole-making of Ti-6Al-4V and CFRP. *Materials* **2021**, *14*, 795. [[CrossRef](#)]
11. Li, Y.X.; Jiao, F.; Zhang, Z.Q.; Feng, Z.; Bin, Y.; Niu, Y. Research on entrance delamination characteristics and damage suppression strategy in drilling CFRP/Ti6Al4V stacks. *J. Manuf. Process.* **2022**, *76*, 518–531. [[CrossRef](#)]
12. Eliseev, A.; Kolubaev, E. Friction drilling: A review. *Int. J. Adv. Manuf. Technol.* **2021**, *116*, 1391–1409. [[CrossRef](#)]
13. Miller, S.F.; Blau, P.J.; Shih, A.J. Microstructural alterations associated with friction drilling of steel, aluminum, and titanium. *J. Mater. Eng. Perform.* **2005**, *14*, 647–653. [[CrossRef](#)]
14. Dehghan, S.; Ismail, M.I.S.; Ariffin, M.K.A.M.; Baharudin, B.T.H.T. Friction Drilling of Difficult-to-Machine Materials: Workpiece Microstructural Alterations and Tool Wear. *Metals* **2019**, *9*, 945. [[CrossRef](#)]
15. Pangjundee, T.; Muttamara, A. Influence of process parameters in friction drilling of titanium Ti-6Al-4V alloy. *MM Sci. J.* **2021**, *2021*, 4791–4796. [[CrossRef](#)]
16. Kumar, A.; Bhardwaj, R.; Joshi, S.S. Thermal modeling of drilling process in titanium alloy (Ti-6Al-4V). *Mach. Sci. Technol.* **2020**, *24*, 341–365. [[CrossRef](#)]
17. Kumar, R.; Hynes, N.R.J. Numerical analysis of thermal drilling technique on titanium sheet metal. In Proceedings of the 2nd International Conference on Condensed Matter and Applied Physics (ICC 2017), Bikaner, India, 24–25 November 2017.
18. Sam Froes, F.H. *Titanium in Medical and Dental Applications*; Woodhead Publishing: Swanson, UK, 2018.
19. *ASTM B265-15*; Standard Specification for Titanium and Titanium Alloy Strip, Sheet, and Plate. American Society for Testing and Materials: West Conshohocken, PA, USA, 2015.
20. Eswara Prasath, N.; Selvabharathi, R. Influence of Plasma Transfer Arc Cladding of NiCrBFe filler powder on microstructure and tensile properties of Titanium Grade 2 and Ti 6Al-4V alloy dissimilar joint prepared by laser beam welding. *Opt. Laser Technol.* **2020**, *128*, 106206. [[CrossRef](#)]
21. Contieri, R.J.; Zanotello, M.; Caram, R. Recrystallization and grain growth in highly cold worked CP-Titanium. *Mater. Sci. Eng. A* **2010**, *527*, 16–17. [[CrossRef](#)]
22. Eliseev, A.A.; Fortuna, S.V.; Kolubaev, E.A.; Kalashnikova, T.A. Microstructure modification of 2024 aluminum alloy produced by friction drilling. *Mater. Sci. Eng. A* **2017**, *691*, 121–125. [[CrossRef](#)]
23. Eliseev, A.A.; Kalashnikova, T.A.; Fortuna, S.V. Structure of AA5056 after friction drilling. In Proceedings of the International Conference on Advanced Materials with Hierarchical Structure for New Technologies and Reliable Structures 2017 (AMHS'17), Tomsk, Russia, 9–13 October 2017.
24. Hamzawy, N.; Mahmoud, T.S.; El-Mahallawi, I.; Khalifa, T.; Khedr, M. Optimization of Thermal Drilling Parameters of 6082 Al-Alloy Based on Response Surface Methodology. *Arab. J. Sci. Eng.* **2023**, *48*, 12001–12014. [[CrossRef](#)]
25. Policena, M.R.; Trindade, A.; Fripp, W.H.; Israel, C.L.; Fronza, G.; de Souza, A.J. Fatigue failure analysis of HSLA steel sheets holed by conventional and flow drilling processes. *Rev. Mater.* **2019**, *24*, e12468.

Disclaimer/Publisher's Note: The statements, opinions and data contained in all publications are solely those of the individual author(s) and contributor(s) and not of MDPI and/or the editor(s). MDPI and/or the editor(s) disclaim responsibility for any injury to people or property resulting from any ideas, methods, instructions or products referred to in the content.